Academic Article

Use of local age of air to study the relation between ventilation efficiency and building configuration

Franchesca G. Gonzalez O.*[1] Tomohito Matsuo*[1] Hikari Shimadera*[1] Akira Kondo *[1]

*[1] Graduate School of Engineering, Osaka University

Corresponding author: Franchesca G. GONZALEZ O., franchesca@ea.see.eng.osaka-u.ac.jp

ABSTRACT

Since human population living in urban areas has been increasing rapidly, strategies to reduce the urban heat island effect are becoming more crucial. It is well-known that appropriate ventilation designs where the wind is able to blow away local heat and pollution accumulation might help with the situation. This paper uses the concept of the local age of air, defined as the time taken by fresh air to replace old air after it enters to a given zone, to evaluate the relation between ventilation efficiency and building configurations. For this purpose, CFD simulations were carried out by using OpenFOAM, the calculation domain was set to x: 1000 m, y: 1000 m, z: 180 m and the actual building site was defined as x: 355 m y: 365 m, z: 180 m. Results showed that in complex locations with a large number of buildings the local age of air is higher than that in contrasting locations. Additionally, it was found that some urban parameters, such as the ratio of the area that is not occupied by any building, improve the ventilation efficiency.

Key Words: Urban heat island, Ventilation efficiency, Local age of air, CFD

1. Introduction

Nowadays, with over 50% of the human population living in cities [(1)], urban planning is facing many challenges, such as the reduction in the difference of the temperature observed between cities and surrounding areas, known as urban heat island [(2)]. Some studies have already identified that the natural wind coming from areas surrounding the cities plays an important role in the city ventilation. For example, Hsieh et al. [(3)] have shown the benefits of the wind corridors in urban areas in summer considering the influence of the temperatures according to land use.

In spite of some authors have stated that the heat island formation could be reduced by city ventilation, the identification of urban parameters that improves the outdoor ventilation requires further investigations. Consequently, Wong et al. [(4)] have studied the concept of building frontal area index to describe those paths where the wind can refresh the urban environment. Moreover, Gat and Unger [(5)] have used an urban roughness mapping method to detect potential ventilation path.

Other studies have discussed the implementation of indoor buildings ventilation concepts such as the local age of air to evaluate the ventilation efficiency in cities. Buccolieri et al. [(6)], under the assumptions that the ventilation processes can be describe by the same concepts in outdoors and indoors, and the efficiency of the ventilation does not depend on the scale of turbulence and vertical transport, introduced the concept of the local age of air and flow rate to analyze in terms of ventilation efficiency the city breathability and the pollutant removal within idealized cities. Likewise, Hang and Li [(7)] considered how rural winds transport relatively clean air into high–rise urban areas to dilute airborne pollutants, using air exchange efficiency and the age of air concepts. This paper also takes into account the assumptions stated in those studies and extends the concept of local age of air to configurations of actual cities.

The purpose of this study is to show the suitability of local age of air concept to determine ventilation performance in existing urban environments. Furthermore, it is aimed to discover the relation between the complexity of actual cities and ventilation efficiency, by identifying some parameters involve in the ability of the wind to refresh the urban thermal environment.

2. Methodology

2.1 Calculation condition

In order to evaluate the ventilation efficiency, computational fluid dynamics (CFD) simulations were conducted with OpenFOAM version 4.0, a general-purpose CFD toolbox. In the simulations, three-dimensional incompressible steady-state flow and isothermal condition were assumed. The conservation equations of mass and momentum, and the scalar transport equation were discretized by finite volume method. The standard k-ε model was employed as the turbulence model. The second-order upwind scheme was used as the discretization scheme of the convection terms, and the second-order central difference scheme was used as the discretization scheme of the diffusion terms in the governing equations. The first order Euler method was utilized as time discretization scheme for the scalar transport equation. The SIMPLE algorithm was employed as the pressure-velocity coupling algorithm. The size of the computational domain was x: 1000 m, y: 1000 m, z: 180 m as shown in Figure 1, where approximately 3.4 million of hexahedral cells were generated.

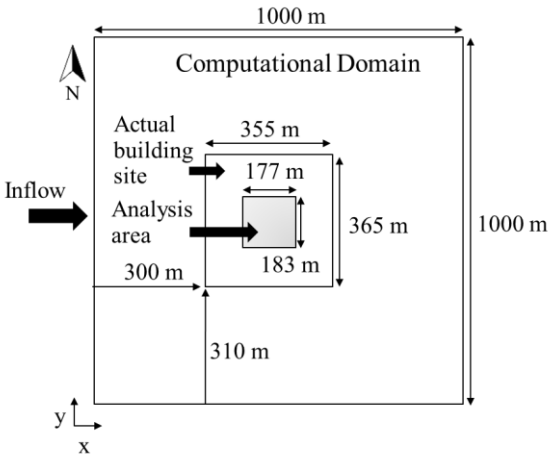

Fig. 1 Top view of the computational domain used in all the studied cases.

The grid resolution in the actual building site was 2.5 m in both of x- and y-direction, outside this area the grid resolution had an increase of 10%.

In z-direction, the grid resolution was 0.5 m until the height of 20 m, and from 20 m an increase of 10% was used until reach the limit of the domain.

For the boundary condition of the wind, the no-slip boundary condition and the symmetry boundary condition were used at all the solid surfaces and at the top, north, and south boundaries of the domain, respectively. At the east (outlet) boundary, the zero gradient boundary condition was set and at the west (inlet) boundary, the power law boundary condition was used. By the power law condition, the inlet wind velocity U at height Z was given as,

$$U = U_{ref}\left(\frac{Z}{Z_{ref}}\right)^{n} \tag{1}$$

where U_{ref} is the reference wind velocity, Z_{ref} is the reference height, and n is the empirically known constant. In this study, 3.0 m/s from the west, 10 m and 0.25 were used as U_{ref}, Z_{ref} and n, respectively.

In the following sections, the wind velocity expressed by the normalized wind velocity U_n was used and defined as,

$$U_n = \frac{U}{U_{ref}} \tag{2}$$

The inlet boundary conditions of the turbulent kinetic energy k, and the dissipation rate ε were decided according to the equations 3, 4 [8] given as,

$$k = \frac{3}{2}(U_{in} \cdot T)^2 \tag{3}$$

$$\varepsilon = C_{\mu}^{\frac{3}{4}} \cdot \frac{k^{\frac{3}{2}}}{l} \tag{4}$$

where U_{in} is the inlet velocity, T is the turbulent intensity, C_{μ} is the constant value, and l is the mixing length. In this study, it was assumed that the turbulence intensity is 0.15 and the mixing length is 1.0 m. The turbulent Schmidt number of 0.9 was used as mentioned in Tominaga et al. [9].

2.2 Real city configuration study

To assess the ventilation efficiency in actual cities with contrasting configuration, Figure 2 shows Hiranomachi study area (34.69N, 135.50E) and Maishima study area (34.66N, 135.40E) both located in Osaka City, Osaka Prefecture Japan.

The length, width, and a number of floors of every building were obtained by the results of the survey on land use conducted by Osaka City in 2005.

Figure 1 and Figure 2 are the top view of the actual building site (x: 355 m y: 365 m) and the analysis area (x: 177 m y: 183 m) in both locations.

In Hiranomachi and Maishima urban environments, an average concentration was defined within the analysis area domain (x: 177 m y: 183 m z: 4 m). This analysis domain was defined based on the consideration of the lowest building height (4 m) and the impact to pedestrian. In these domains, an initial concentration of tracer gas was set to be 1 mg/m^3. Since we want to know the ability of the surrounding wind to remove the contaminants from the analysis area, an initial concentration of tracer gas of 0 mg/m^3 was assumed in the entire domain, excluding the analysis area domain. As same as the wind speed, the normalized concentration C_n is used in the following sections.

$$C_n = \frac{C}{C_{init}} \tag{5}$$

where the C_{init} is the initial concentration 1 mg/m^3.

The time variance of the concentration field of tracer gas in the analysis area domain was calculated to obtain the local age of air.

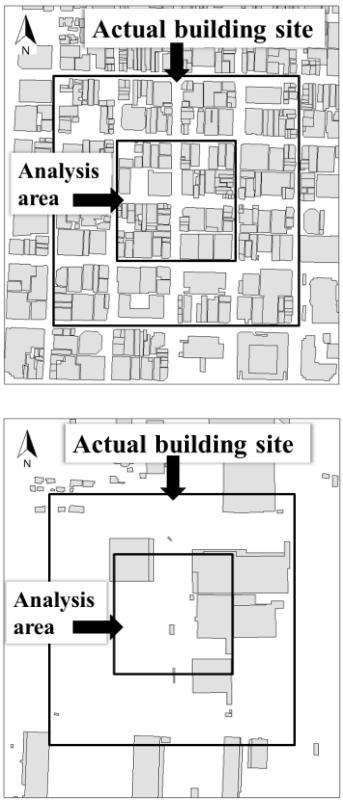

Fig. 2 Hiranomachi area, Osaka City (Top)
Maishima area, Osaka City (Bottom)

The local age of air *LAA* is defined as the time taken by fresh air to replace old air after it enters to a given zone and is mathematically expressed by equation 6.

$$LAA = \frac{\int_0^\infty t \cdot C_p(t)dt}{\int_0^\infty C_p(t)dt} \tag{6}$$

where C_p is the concentration spatially averaged in the analysis area domain, and t is the time. Important to notice, since in practice we cannot integrate t from zero to infinite, we calculated the local age of air by integrating t from 0 to 1000 s.

2.3 Systematic analysis

Besides the study in Hiranomachi and Maishima, a systematic study of four cases in two different scenarios was carried out to show the parameters influencing the ventilation efficiency for dense urban environment configuration. All the calculation conditions were the same as those used in real city configuration study, the initial concentration of tracer gas was also located in the analysis area domain (x: 177 m y : 183 m z: 4m).

Four arrangements with differents shapes (sixteen cubic buildings, nine cubic buildings, four cubic buildings, and one cubic building) were used and the volume of the buildings for all for configurations was approximated as much as possible to keep the same volume as Hiranomachi area (496900 m^3).

Scenario No. 1 consisted in the analysis area surrounded by other buildings, as shown in Figure 3; and in the scenario No. 2 the analysis area is isolated.

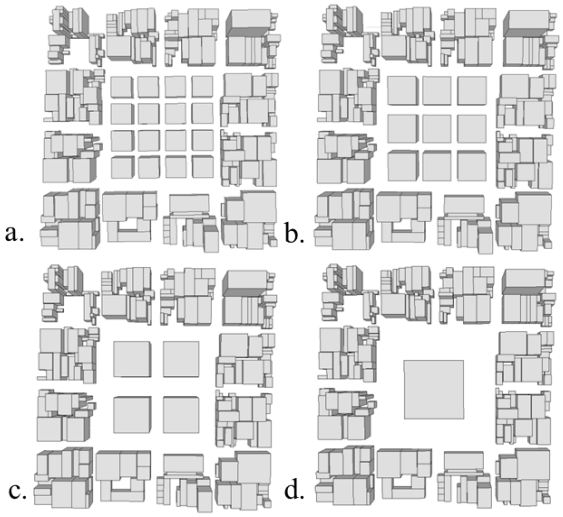

Fig. 3 Representation of the systematic analysis for scenario No. 1; a. sixteen buildings (every building 30 m x 30 m x 30 m), b. nine buildings (every building 40 m x 40 m x 40 m), c. four buildings (every building 50 m x 50 m x 50 m), and d. one building (80 m x 80 m x 80 m)

3. Results and discussion

3.1 Real city configuration study

As we can see in Figure 4, the wind profile in Hiranomachi area is lower in downstream; especially streets perpendicular to x-axis, in the center of the analysis area domain, the normalized velocity U_n ranges from 0.0 to 0.4.

In Maishima area, on the other hand, U_n is around 0.4, and within the analysis area, the wind velocities are apparently higher than 0 m/s.

From Figure 4b, the wind in Hiranomachi is much lower than Maishima. This remarkable difference between Hiranomachi and Maishima is the result of the morphology. For example, the height of the buildings ranges from 4 m to 52 m in Hiranomachi, and from 4 m to the highest building of 20 m at Maishima.

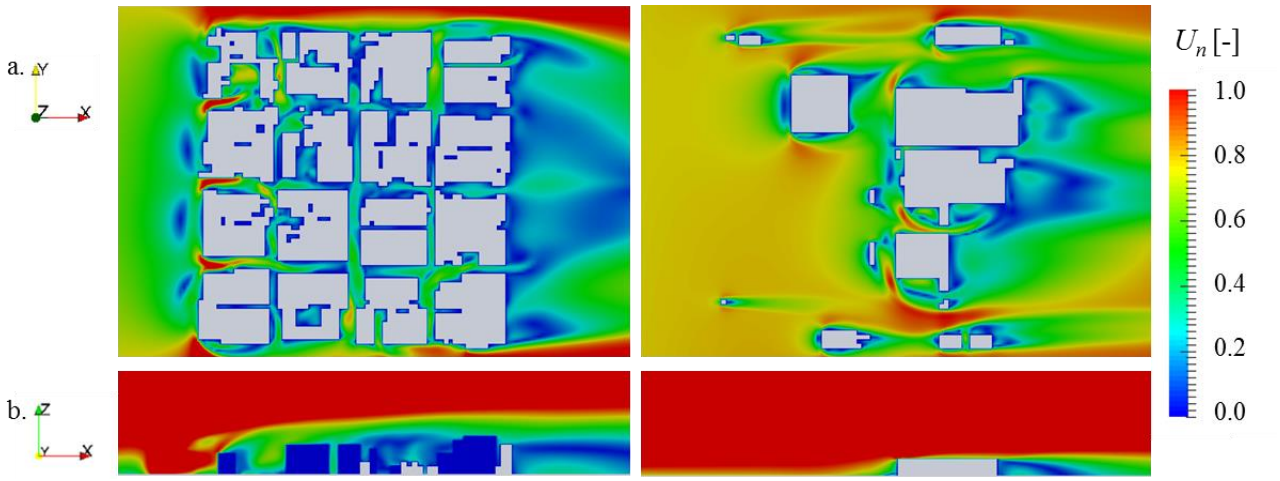

Fig. 4 Actual building site wind profile U_n [-] for Hiranomachi (left) and Maishima (right): a. Top views at z: 1 m, b. Lateral views at y: 500 m

Figure 5 illustrates the concentration fields in Hiranomachi and Maishima analysis area domain where a large amount of the tracer gas was blown off in the first few minutes, nevertheless, some of the tracer gas has been retaining in areas surrounded by buildings in Hiranomachi. The main reason may be the low wind speed and the complicated building shapes. Therefore, the local age of air in Hiranomachi (147 s) is almost three times higher than Maishima (49 s).

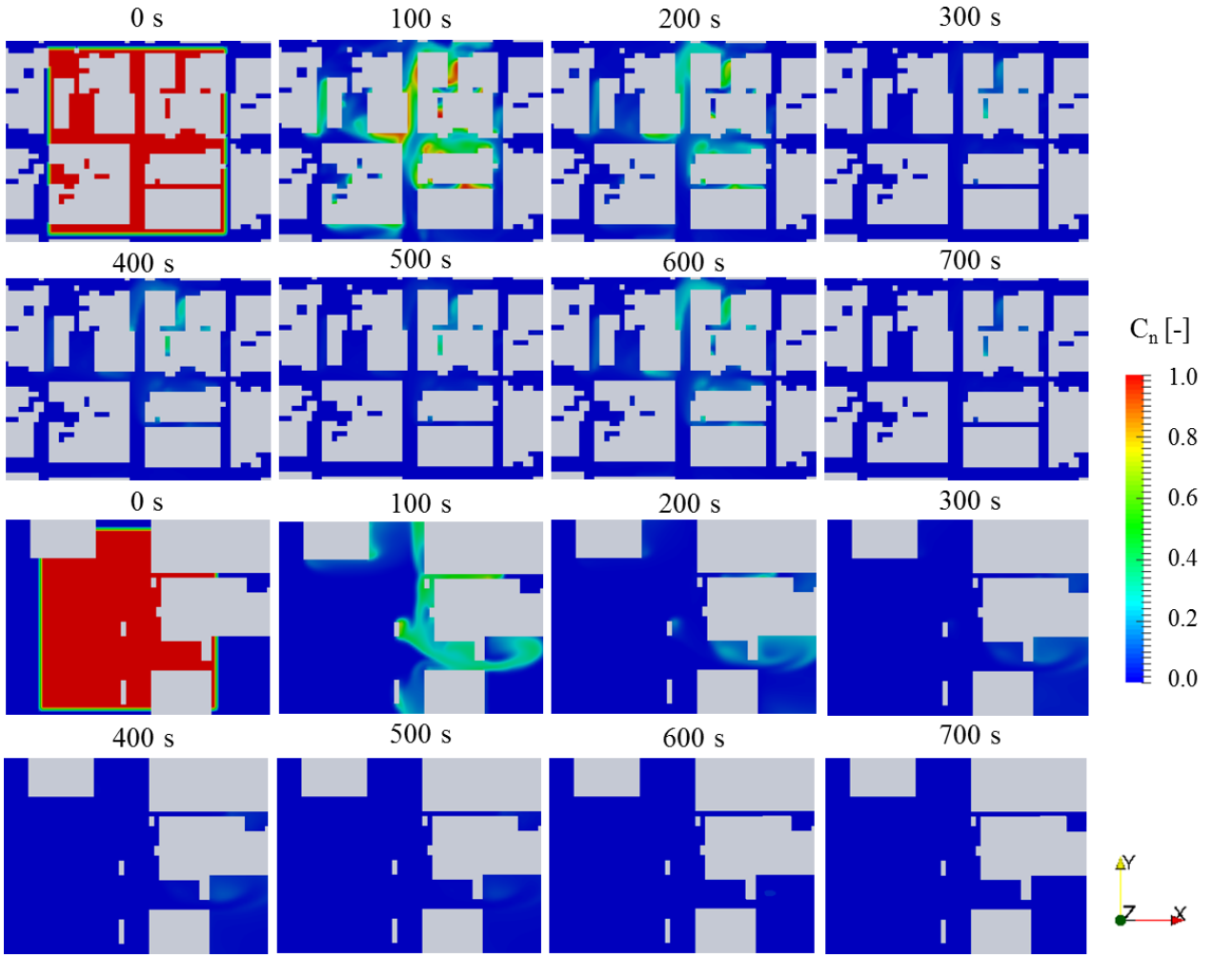

Fig. 5 Concentration field at z: 1 m for Hiranomachi analysis area (upper rows) and Maishima analysis area (bottom rows), in the interval of time from 0 s to 700 s.

Figure 6 shows the spatially averaged concentration in analysis area domain versus time in Hiranomachi and Maishima. The average concentration in Maishima decreases much faster than Hiranomachi, because of the higher wind velocity in the analysis area domain.

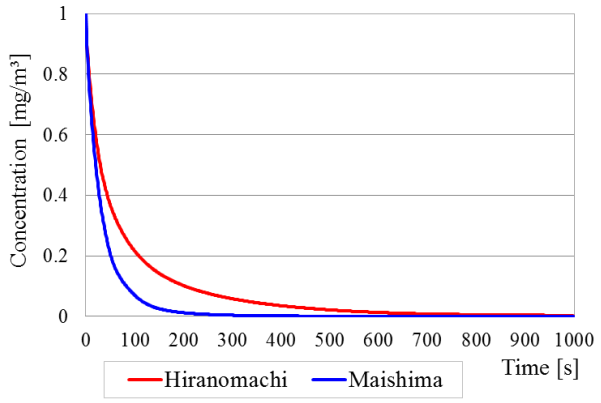

Fig. 6 Spatially averaged concentration vs time in Hiranomachi and Maishima.

These results show that complex geometry causes lower ventilation efficiency by lower wind speed and many drifts.

3.2 Systematic analysis

Figure 7 and Figure 8 show the time variance of the concentration field and the local age of air for all the cases in both scenarios, respectively. From the comparison of the scenarios, it can be said that the tracer gas was removed more easily when the buildings are isolated, because the absent of surrounding buildings allows the wind to reach the analysis areas with large velocity and less eddies. Moreover, there is a more symmetric wind flow pattern in x-direction for cases under scenario No 2. This indicates that complicated wind pattern caused by complex geometry may degrade the ventilation efficiency. The cases of sixteen buildings, however, show a different behaviour, in which the result of scenario No. 2 indicates the value of the local age of air to be a slightly higher. This may be explained as follows: the wind mainly blows west to east for scenario No.2, so that causes lower wind speed in the street which runs from the north to the south direction; moreover, the turbulence of the wind is smaller in the case of sixteen buildings in scenario No.1 than scenario No. 2, because of no surrounding buildings; as a result, the tracer gas remains in the street that runs from north to south direction. In addition, sixteen cases have the smallest street width, so that the wind is not able to enter into the streets.

It can be said, from the comparison of the values of local age of air for the arrangements in scenario No.1, which the ventilation efficiency depends on not only the number of building because local age of air in the case of sixteen buildings is lower than the case of nine buildings.

As shown in Figure 7, though the concentration near the perimeter of the analysis area decreases inmediately, the concentration on the leeward of a building decrease slowly. The former can be explained by the convection, and the latter may be related with the phenomena of the turbulent flow such as eddies and separated flow.

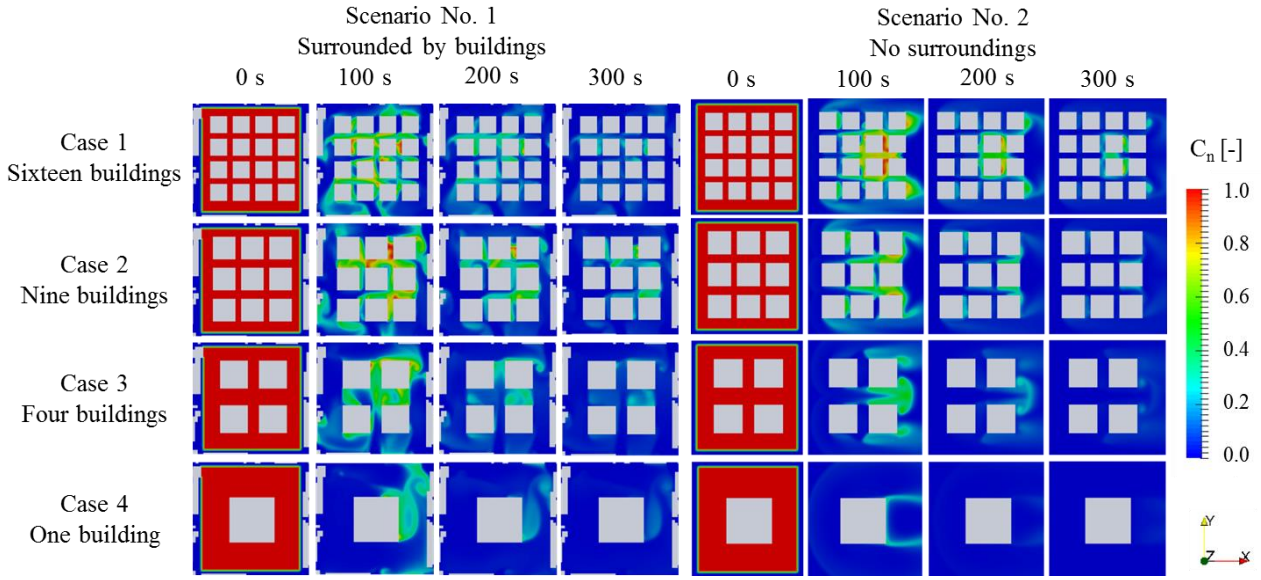

Fig. 7 Concentration field at z: 1 m for Case 1, Case 2, Case 3 and Case 4 in both scenarios; scenario No. 1 surrounded by buildings and scenario No. 2 no surroundings, in the interval of time from 0 s to 300 s.

Additionally, we defined the open space ratio r_{os} as,

$$r_{os} = \frac{A_{os}}{A_{aa}} \tag{7}$$

where, A_{os} is the free area that is not occupied by any building and the A_{aa} is analysis area (177 m x 183 m). We found that open space ratio has a relationship with the local age of air. Actually, Figure 8 shows that those cases where open space ratio was bigger the local age of air was lower. For the study of the real city configuration, we can confirm that the open space ratio is directly related with the local age of air.

However, more consideration is required because the both of sixteen and nine buildings cases, which have almost same open space ratio, show different values of the local age of air.

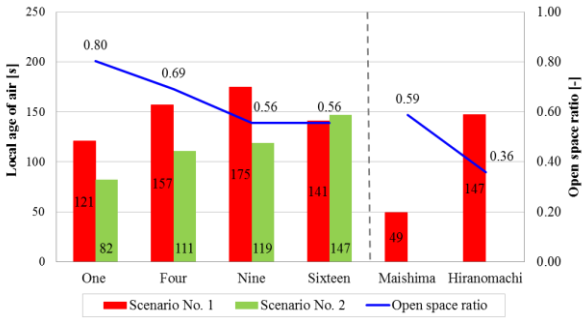

Fig. 8 Local age of air and open space ratio for scenario No. 1, scenario No. 2, Hiranomachi and Maishima.

For future work, other simulations should be conducted in order to clarify, at least in this context, the influence of the geometry, as well as the importance of the turbulent eddies in the removal of pollutants. In general, simulation results show to be in agreement with the fact that urban areas with a large amount of building and irregular configurations have as result poor ventilation.

4. Conclusions

In this contribution, we have demonstrated that the local age of air can be used as index of the ventilation efficiency in urban environments. With all the steps applied in this work, we indicated how the local age of air is used as a tool to analyze the influence of urban morphology on the city ventilation.

In addition, it was found that irregular configurations, buildings height, surroundings, street width and open space ratio have a relationship with the ventilation efficiency. Through the identification of these parameters and the study of their influence, possible modifications or suitable designs of the city spaces can be taken into consideration to help in the urban planning process to reduce the heat island effect.

Acknowledgements

Part of this work was financially supported by the Obayashi Foundation. In addition, we are grateful to Osaka City Government for providing building data from their survey on land use conducted in Osaka City in 2005.

References

(1) United Nations, Department of Economic and Social Affairs, Population Division (2014). World Urbanization Prospects: The 2014 Revision, CD-ROM Edition.

(2) T.R.Oke, City size, and the urban heat island, Atmospheric Environment 7 (1967), pp. 769-779.

(3) C.-M. Hsieh, H.-C. Huang, Mitigating urban heat islands: A method to identify potential wind corridor for cooling and ventilation, Computers, Environment and Urban Systems 57 (2016), pp. 130-143.

(4) M. S. Wong, J. E. Nichol, P. H. To, J. Wang, A simple method for designation of urban ventilation corridors and its application to urban heat island analysis, Building and Environment 45 (2010), pp. 1880-1889.

(5) T. Gal, J. Unger, Detection of ventilation paths using high-resolution roughness parameter mapping in a large urban area, Building and Environment 44 (2009), pp. 198-206.

(6) R. Buccolieri, M. Sandberg, S. Di Sabatino, City breathability and its link to pollutant concentration distribution within urban-like geometries, Atmospheric Environment 44 (2010), pp. 1894-1903.

(7) J. Hang, Y. Li, Age of air and air exchange efficiency in high-rise urban areas and its link to pollutant dilution, Atmospheric Environment 45(2011), pp. 5572-5585.

(8) H. Versteeg, W. Malalasekera, An Introduction to Computational Fluids Dynamics: The Finite Volume Method, Prentice Hall, (2007).

(9) Y. Tominaga, T. Stathopoulos, Turbulent Schmidt numbers for CFD analysis with various types of flowfield, Atmospheric Environment 41 (2007), pp. 8091-8099.

(Received Apr. 28, 2017, Accepted Jul. 7, 2017)